Figures and figure supplements

Impaired spatial learning and suppression of sharp wave ripples by cholinergic activation at the goal location

Przemyslaw Jarzebowski *et al*

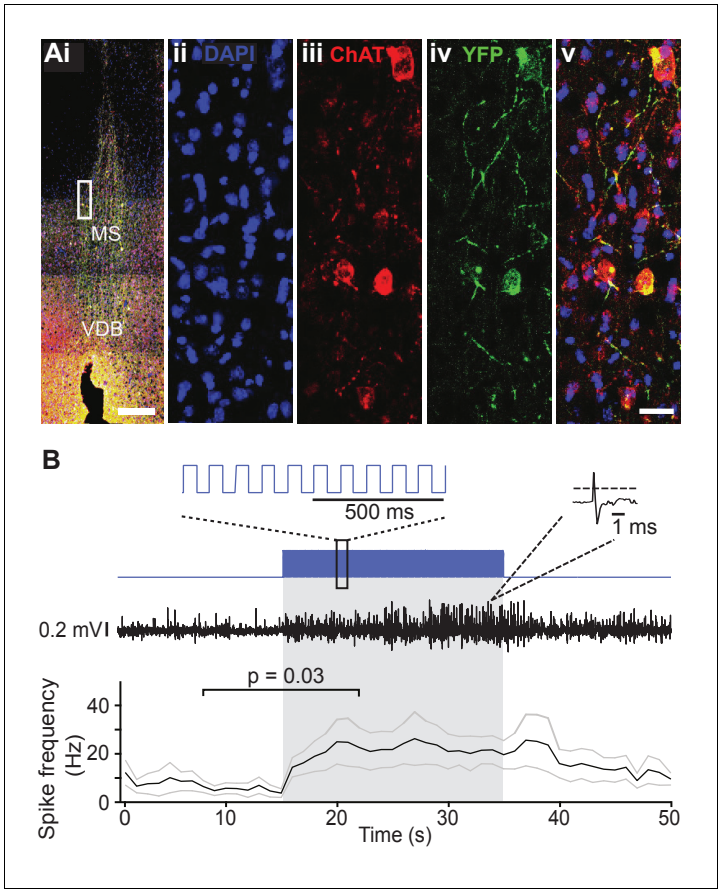

Figure 1. Choline acetyl transferase (ChAT)-Ai32 mice express enhanced YFP-tagged channelrhodopsin-2 (ChR2-eYFP) selectively in cholinergic cells. (**Ai**) Overlay of DAPI, ChAT, and eYFP-positive immunostaining in a coronal section of the medial septum (MS) in a ChAT-Ai32 mouse. Scale bar 500 µm. VDB, ventral diagonal band. (**Aii-v**) Higher magnification of the MS (rectangle in **Ai**), triple immunostaining of DAPI (blue, **ii**), ChAT (red, **iii**), and eYFP (green, **iv**), showing their colocalization (overlay, **v**). Scale bar 50 µm. (**B**) Sample trace of multi-unit recording from the MS in a ChAT-Ai32 mouse. Top: the stimulation protocol (blue) beginning at 15 s. Inset shows a section of the 50-ms-long square stimulation pulses at 10 Hz. Middle: an example recording trace; inset shows an example unit recorded. Bottom: mean spike frequency (n = 6). *p=0.03, two-tailed paired Wilcoxon signed-rank test. Gray lines represent mean ± SEM.

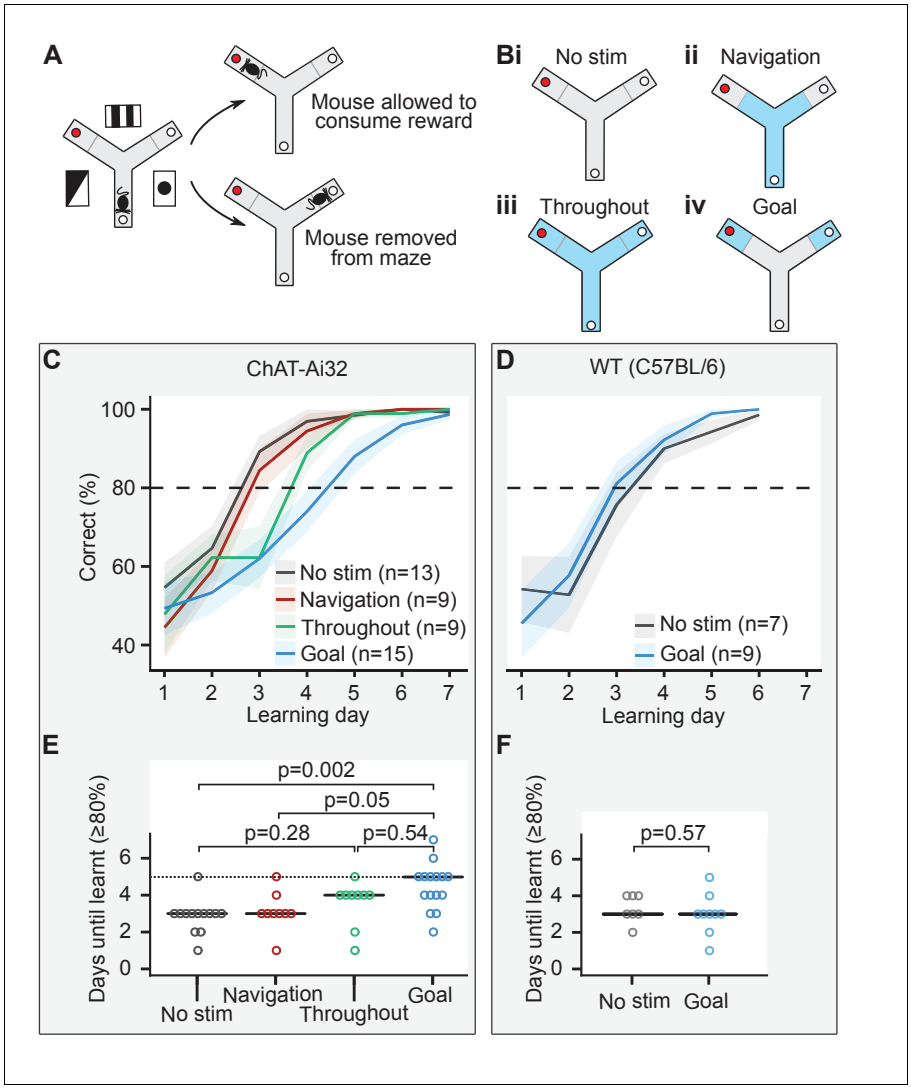

Figure 2. Cholinergic stimulation in the goal zone slows learning of the appetitive Y-maze task. (**A**) Mice were trained on an elevated three-arm maze to find a food reward (red dot) in an arm that remained at a fixed location relative to visual cues in the room. Mice were allowed to consume the reward if they chose the correct arm but were removed from the maze if they chose the incorrect arm. (**B**) Mice were pseudo-randomly split into four groups to test four optogenetic stimulation conditions. Blue indicates stimulation for the four conditions: (i) no stimulation, (ii) stimulation only until the goal zone was reached (gray line), (iii) stimulation throughout the maze, and (iv) stimulation only in goal zone. (**C**) Choline acetyl transferase (ChAT)-Ai32 mice received blocks of 10 trials each day for 7 consecutive days and the number of entries to the rewarded arm was recorded. The performance of all four groups of mice improved with time but at different rates. (**D**) As in (**C**) but for wild-type (WT) mice. (**E**) The number of days required for each group of the ChAT-Ai32 mice to reach the learning criterion of ≥80%. Horizontal bars indicate the median within each group. The p-values for differences between groups were calculated using post hoc Dunn tests. (**F**) As in (**E**) but for WT mice.

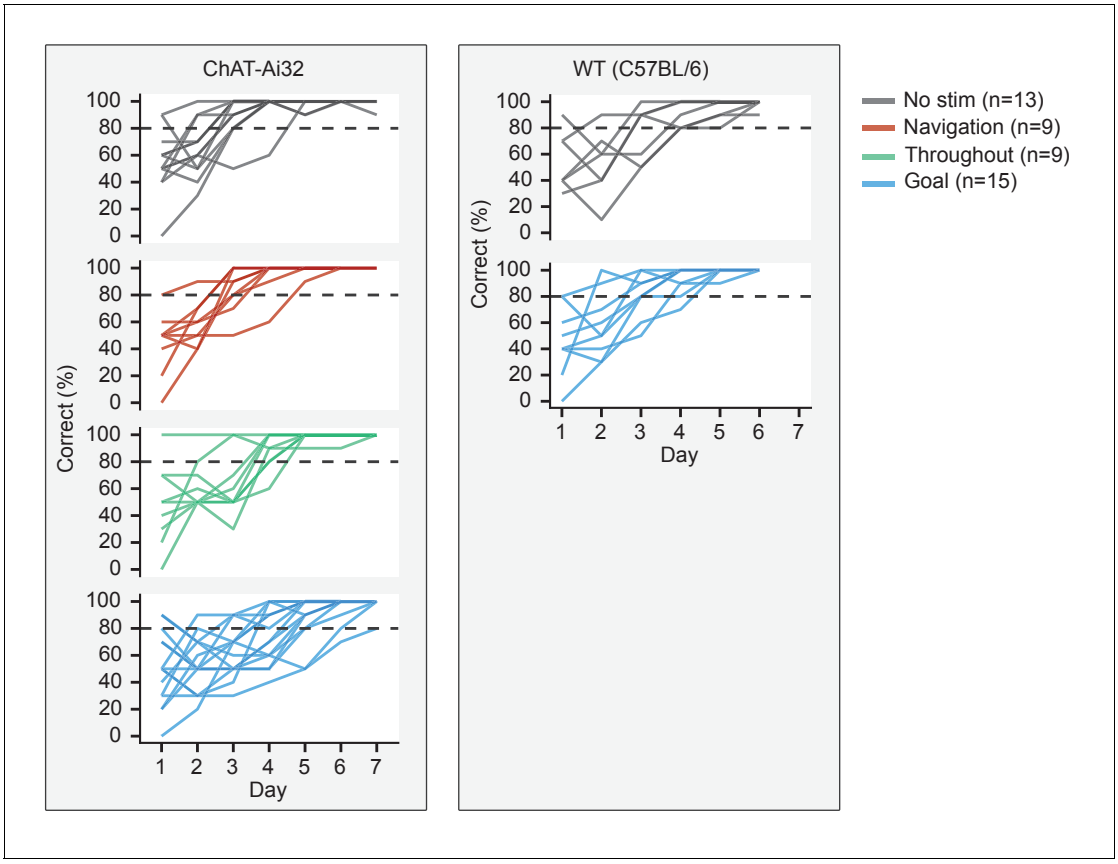

Figure 2—figure supplement 1. Individual learning curves. Learning curves of individual mice that were aggregated to show group differences.

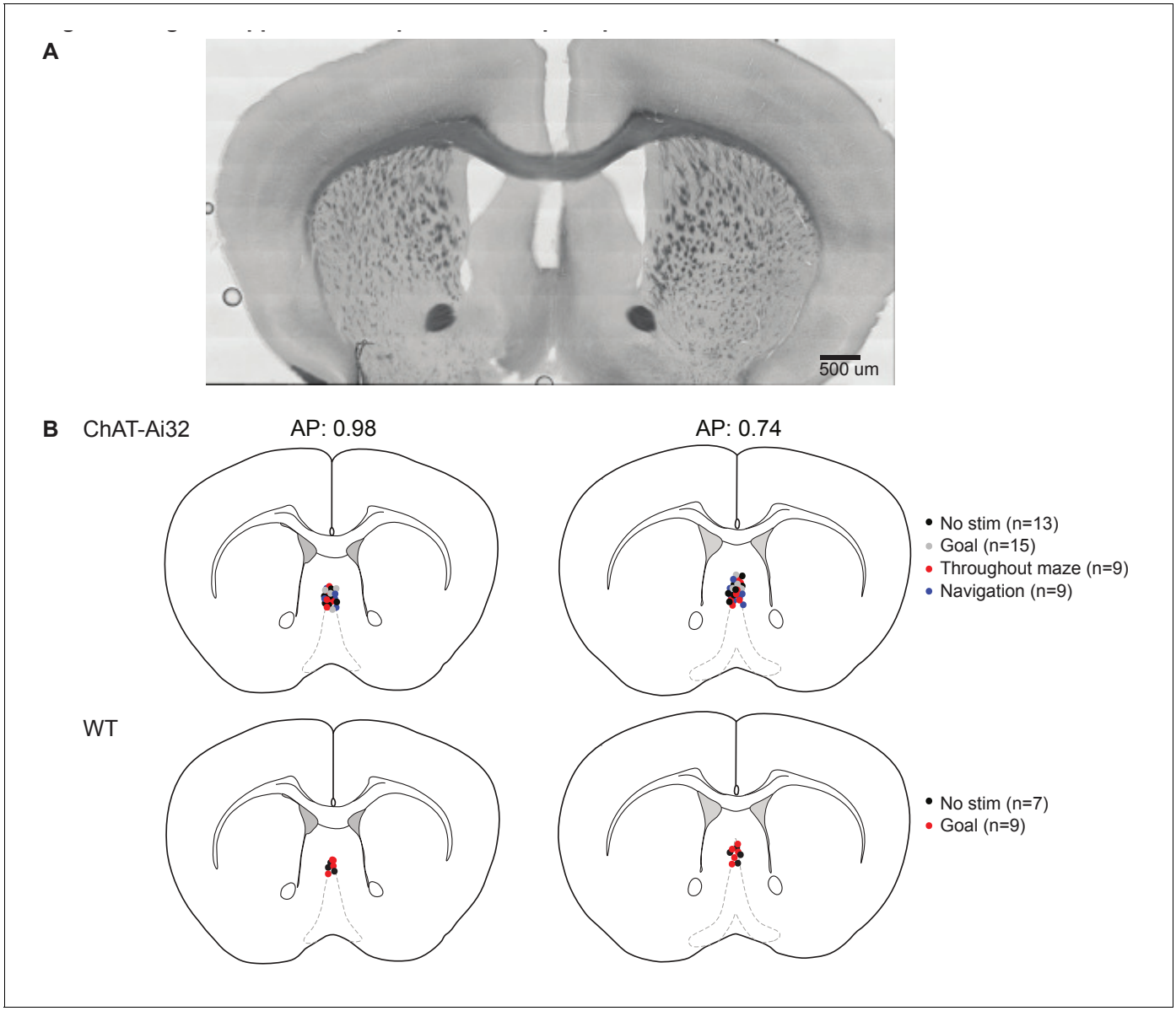

Figure 2—figure supplement 2. Optic fiber implant placement. Implant placement did not vary between experimental groups. After behavioral testing, brains were fixed and sliced, and the placement of the deepest point of the implant was recorded for each mouse. (**A**) Representative bright-field image of the optical implant site over the medial septum. Scale bar 500 µm. (**B**) The approximate locations of the optic fibre implant tip for each mouse.

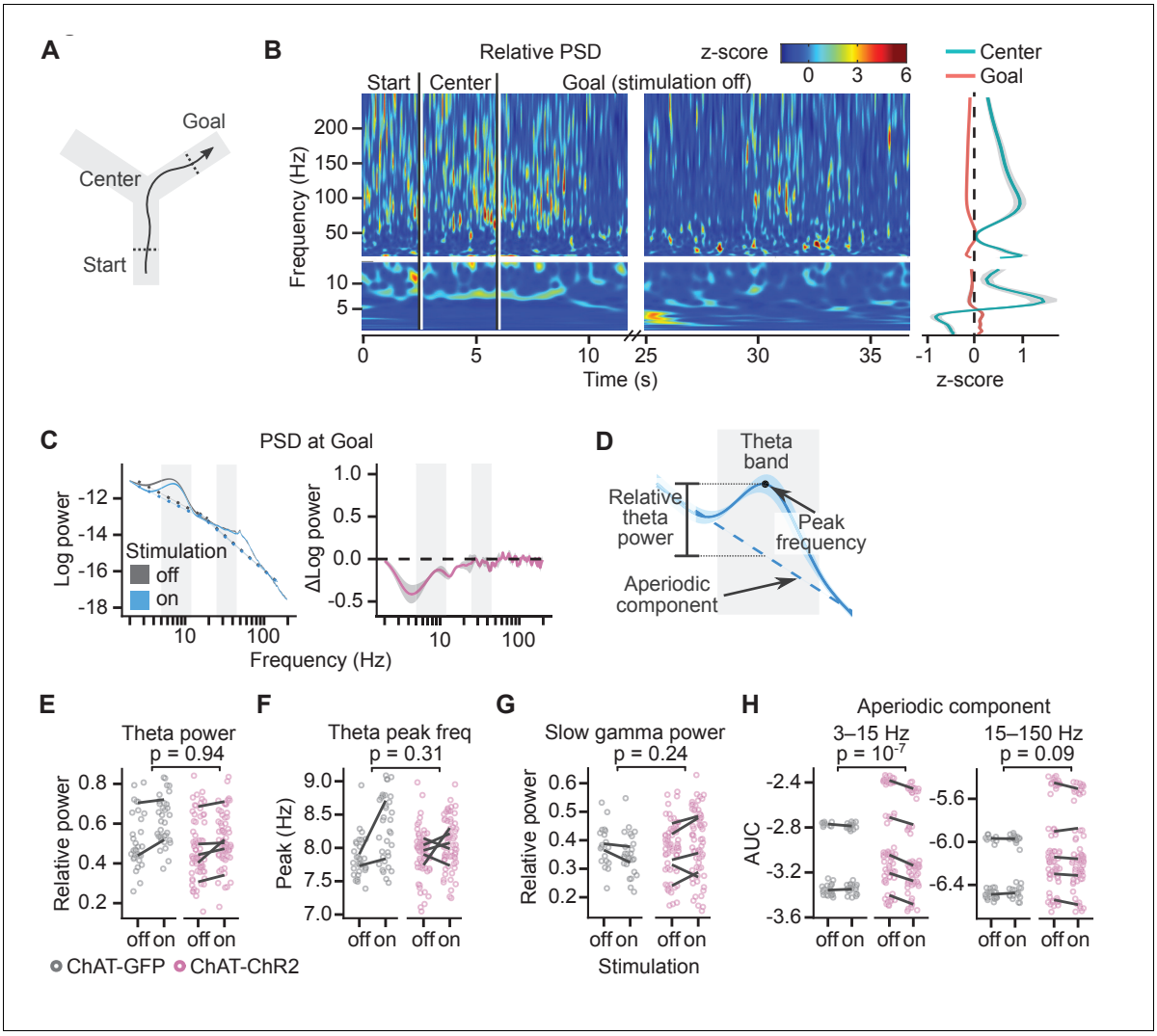

Figure 3. Cholinergic stimulation during the Y-maze task did not change theta-gamma oscillations. (**A**) Schematic showing the maze zones. (**B**) Spectrogram of the local field potential (LFP) recorded in a single non-stimulated trial. The values were z-scored to show relative changes in frequency. Note transient increases in high-frequency power throughout the recording and high theta power at Center. Right: mean z-score value at Center and Goal as a function of frequency. (**C**) Left: power spectral density (PSD) of the LFP recorded from a representative animal on non-stimulated and stimulated-at-Goal rewarded trials. The dashed lines show the fitted aperiodic component. Right: difference in PSD between day-averaged trials with stimulation off and on. Ribbons extend ±1 SEM of log power. Gray background marks the frequency range of theta and slow gamma bands. (**D**) PSD parameters that were assessed for the stimulation effect: relative theta power (**E**), spectral peak frequency in the theta band (**F**), slow gamma power (**G**), and the aperiodic component (**H**). The aperiodic component was fitted for two frequency ranges, 3–15 and 15–150 Hz, and compared using the area under curve (AUC). (**E–H**) Values plotted for individual trials. Lines connect means for individual animals. p-values were calculated with linear mixed-effects models for the interaction of mouse group–laser effects.

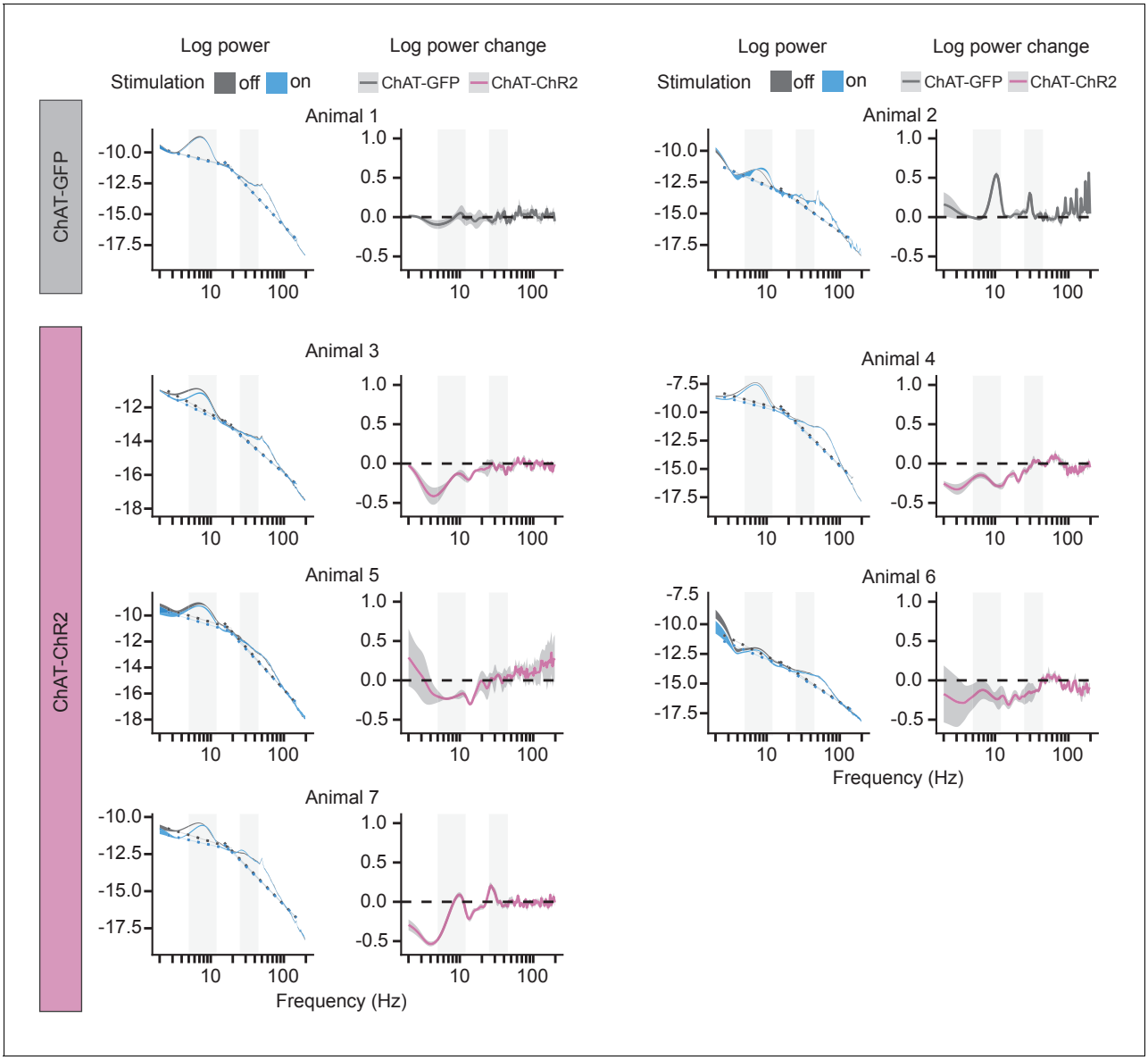

Figure 3—figure supplement 1. Power spectral density (PSD) at Goal location. For each mouse, the left panel shows mean PSD ± 1 SEM in rewarded trials with the stimulation off and on. Dashed lines show fitted aperiodic component. The right panel shows difference between log power calculated on day-averaged trials with the stimulation off and on as a function of frequency. Gray background marks the frequency range of theta and slow gamma bands.

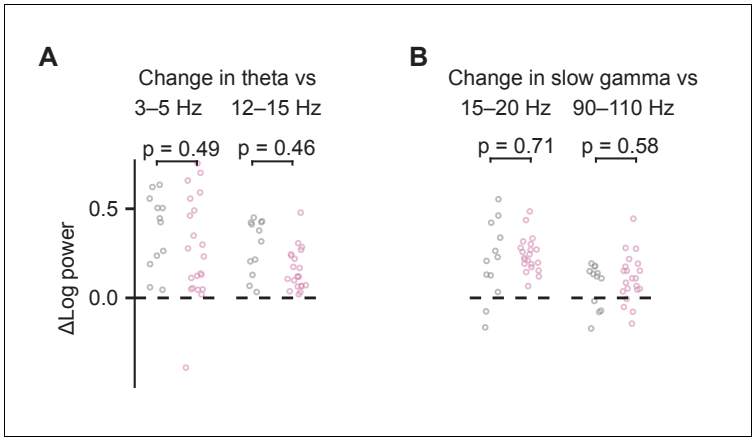

Figure 3—figure supplement 2. Power spectral density (PSD) change of theta and slow gamma at Goal location vs. neighboring frequency band. (**A**) Change in theta power as the result of optogenetic stimulation compared to change in surrounding frequency bands. (**B**) As in (**A**) but for slow gamma power. Values are shown for log power differences in day-averaged trials with stimulation off and on. p-values were calculated with linear mixed-effects models for the effect of the mouse group (ChAT-ChR2 vs. ChAT-GFP).

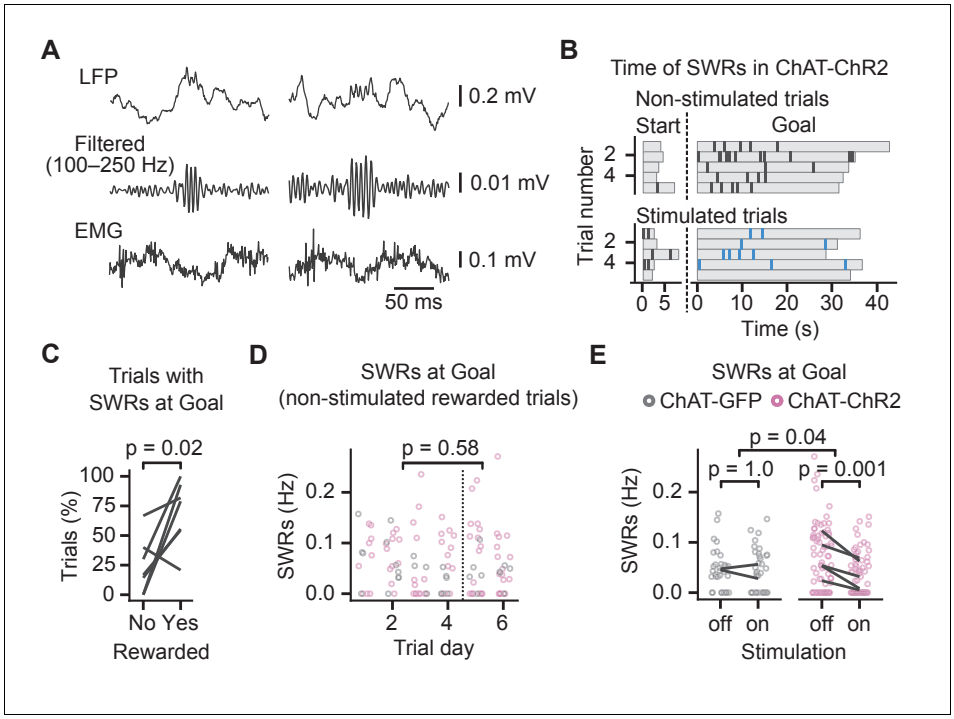

Figure 4. Cholinergic stimulation during the Y-maze task reduced incidence of sharp wave ripples (SWRs). (**A**) Example SWRs recorded at the Goal location: local field potential (LFP) traces (top), the same traces after 100–250 Hz bandpass filtering (middle), and simultaneously recorded electromyography (EMG) (bottom). (**B**) Time of SWRs recorded from a representative mouse over multiple trials the same day. Time measured relative to the trial start and arrival at Goal. Stimulated and non-stimulated trials are grouped for clarity. (**C**) Percentage of trials with SWRs at Goal compared between unrewarded and rewarded non-stimulated trials. One line per animal shown. p-value calculated with paired t-test. (**D**) SWR incidence as a function of trial day. Data shown for choline acetyl transferase (ChAT)-GFP and ChAT-ChR2 mice together, values plotted for individual non-stimulated rewarded trials. Dashed vertical line separates early and late trials. p-value calculated with linear mixed-effects model for the effects of early vs. late trials. (**E**) Effect of cholinergic stimulation on SWR incidence at Goal location in rewarded trials. Data shown for ChAT-GFP and ChAT-ChR2 mice, values plotted for individual trials. Lines connect means per animal. p-values calculated with linear mixed-effects model for the interaction of mouse group–laser effects; groups were compared with post hoc test on least-square means.

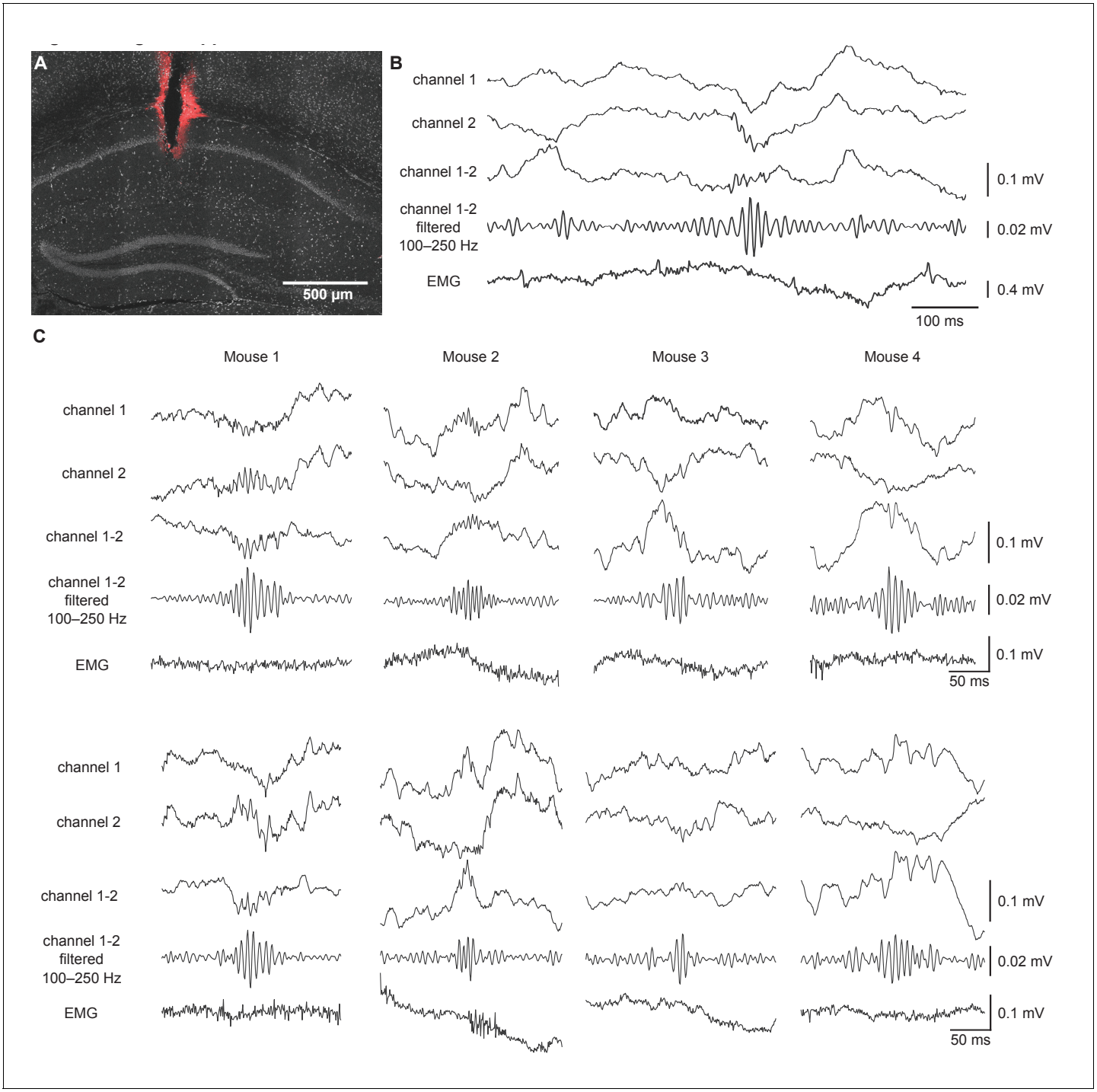

Figure 4—figure supplement 1. Sharp wave ripples (SWRs) recorded at Goal location. (**A**) Location of the recording electrodes in the DAPI-stained image of the CA1. Red DiI stains mark the electrode tracks. Scale bar: 500 µm. (**B**) Local field potential (LFP) signal showing an SWR from wire electrodes placed in the CA1. The top two traces show LFP recorded on two channels, the trace below shows the differential signal by subtraction of Channel 2 from Channel 1. For SWR detection, the subtracted trace was 100–250 Hz bandpass filtered. The bottom trace shows electromyography (EMG) signal with no muscle activity at the time of the SWR. (**C**) Example traces from four mice with LFP signal centered around the time of SWR. Trace order as in (**B**).

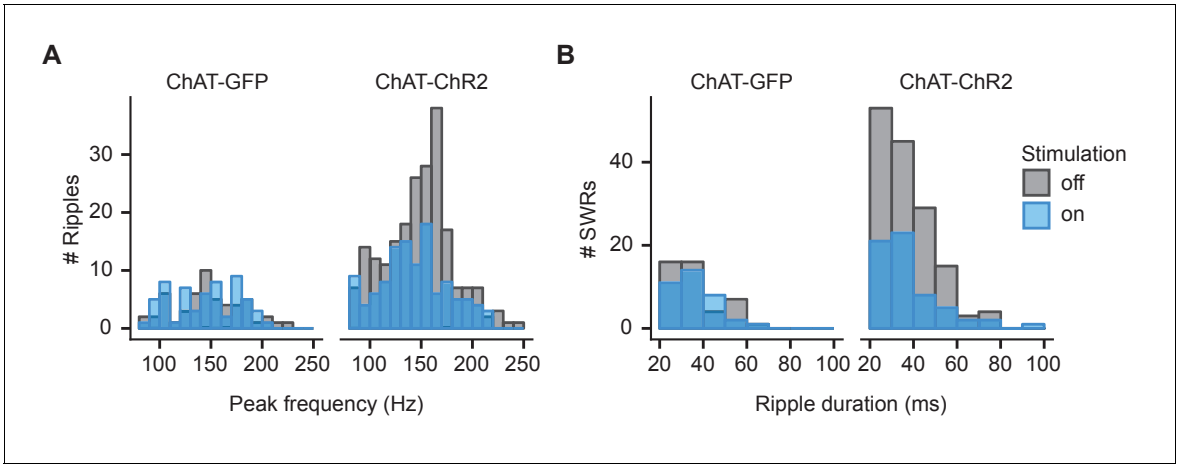

Figure 4—figure supplement 2. Spectral peak frequency of ripples and duration of sharp wave ripples (SWRs) at Goal location. (**A**) Histogram showing spectral peak frequency for all ripples at Goal location compared between stimulated and non-stimulated rewarded trials. (**B**) Histogram showing duration of SWRs (≥140 Hz) at Goal compared between stimulated and non-stimulated rewarded trials.

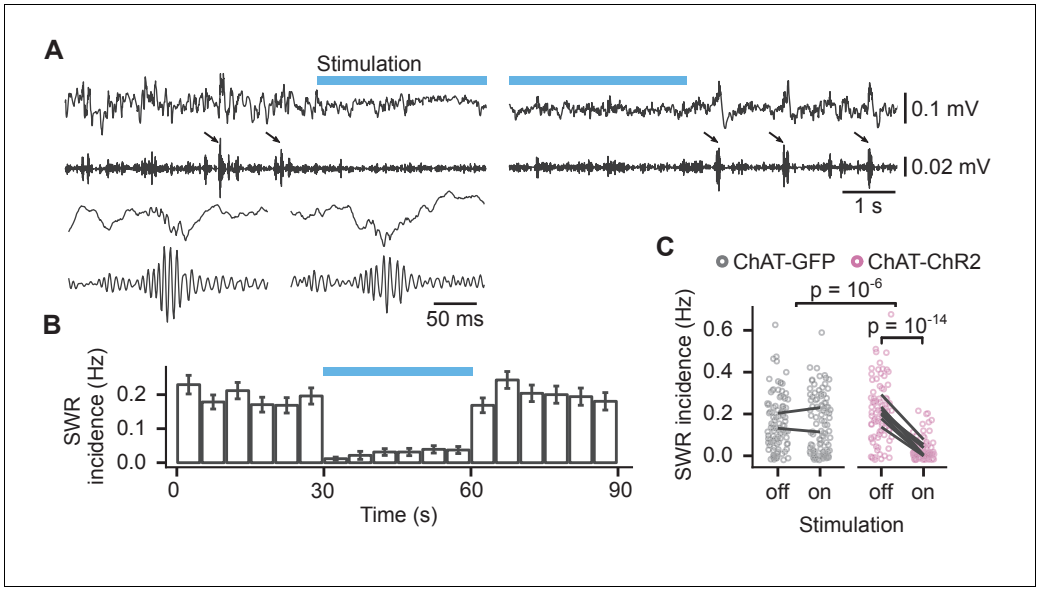

Figure 5. Activation of medial septum cholinergic neurons reduced incidence of sharp wave ripples (SWRs) during sleep. (**A**) Local field potential (LFP) from the CA1 of a sleeping mouse recorded before, during, and after optogenetic stimulation with 100–250 Hz bandpass filtered trace for ripple detection shown below. The detected SWRs are marked with arrows. The inset (lower left) shows two example SWRs at greater time resolution. (**B**) Histogram of SWR incidence before, during, and after 30 s of stimulation with 50-ms-long pulses at 10 Hz (n = 103 epochs from eight ChAT-ChR2 mice). (**C**) Comparison of SWR incidence during the stimulated and non-stimulated epochs for ChAT-GFP and ChAT-ChR2 mice. Lines connect mean incidence in individual mice. p-values were calculated with linear mixed-effects model for the interaction of mouse group–laser effects; groups were compared with post hoc test on least-square means.

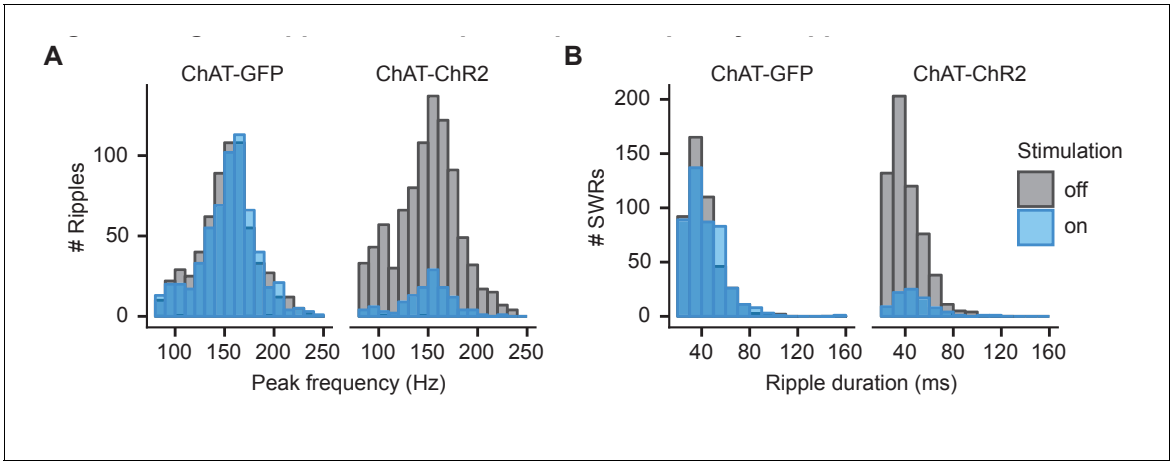

Figure 5—figure supplement 1. Spectral peak frequency of ripples and duration of sharp wave ripples (SWRs) during sleep. (**A**) Histogram showing spectral peak frequency for all sleep ripples in stimulated and non-stimulated epochs. (**B**) Histogram showing duration of SWRs (≥140 Hz) in stimulated and non-stimulated epochs.

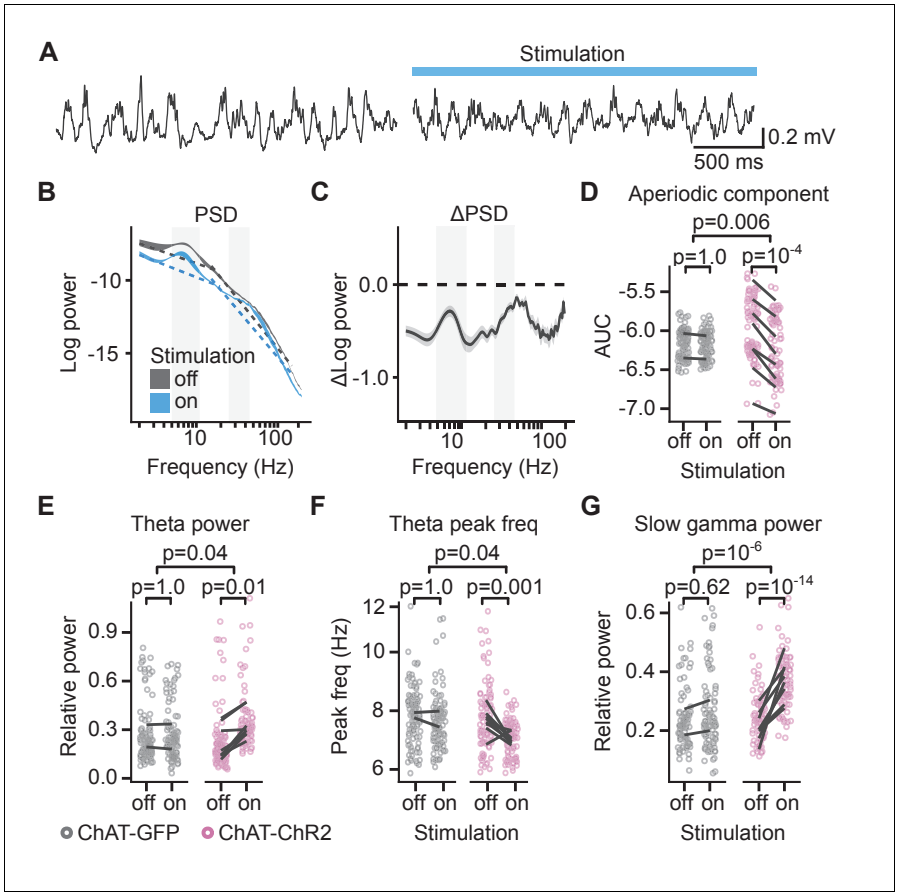

Figure 6. Cholinergic stimulation increased theta and slow gamma activity in sleeping mice. (**A**) Local field potential (LFP) recording from the CA1 of a sleeping mouse recorded without (left) and with (right) optogenetic stimulation. (**B**) Power spectral density (PSD) of the LFP recorded from a single animal during the epochs without and with optogenetic stimulation. Ribbons extend ±1 SEM of PSD. Gray background marks the frequency range of theta and slow gamma bands. The dashed lines show the fitted aperiodic component. (**C**) Difference in PSD between subsequent epochs with stimulation off and on. Data shown for the animal in (**B**). Ribbons extend ±1 SEM of log power. (**D**) Optogenetic stimulation in the choline acetyl transferase (ChAT)-ChR2 mice reduced the power of the aperiodic component in 15–150 Hz frequency range. (**E**) Optogenetic stimulation in the ChAT-ChR2 mice, but not in the ChAT-GFP mice, increased relative theta power, (**F**) decreased spectral peak frequency in the theta band, and (**G**) increased relative slow gamma power. Values were calculated on individual epochs, lines connect means for individual animals. p-values were calculated with linear mixed-effects model for the interaction of mouse group–laser effects; groups were compared with post hoc test on least square means.

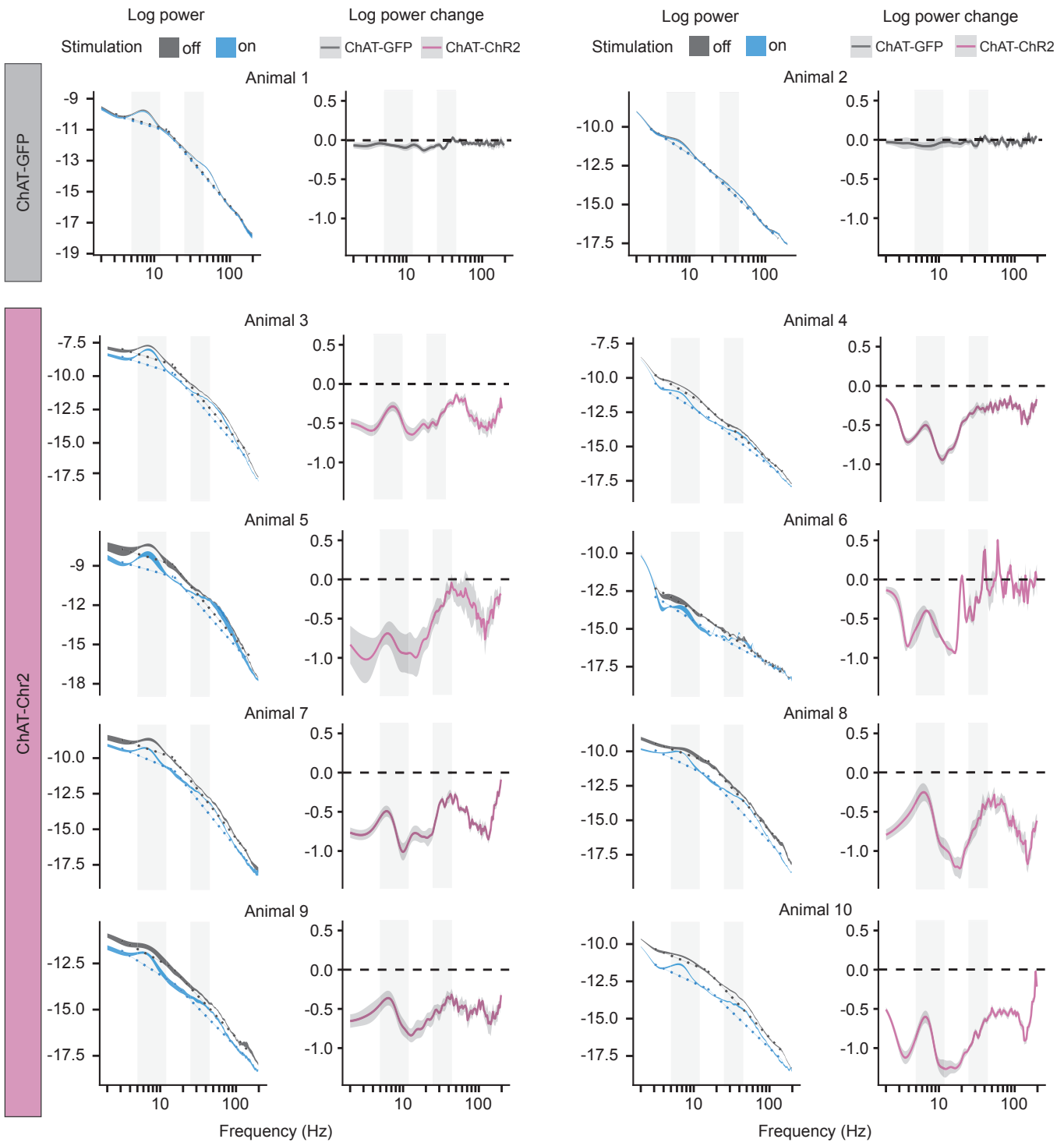

Figure 6—figure supplement 1. Power spectral density (PSD) of local field potential (LFP) in individual sleeping mice. PSD of the LFP and its change during sleep epochs without and with optogenetic stimulation shown in each animal. The left panel shows PSD ± 1 SEM and the dashed lines show fitted aperiodic component; the right panel shows difference between log power calculated on subsequent epochs with stimulation off and on as a function of frequency. Ribbons extend ±1 SEM. Gray background marks the frequency range of theta and slow gamma bands.

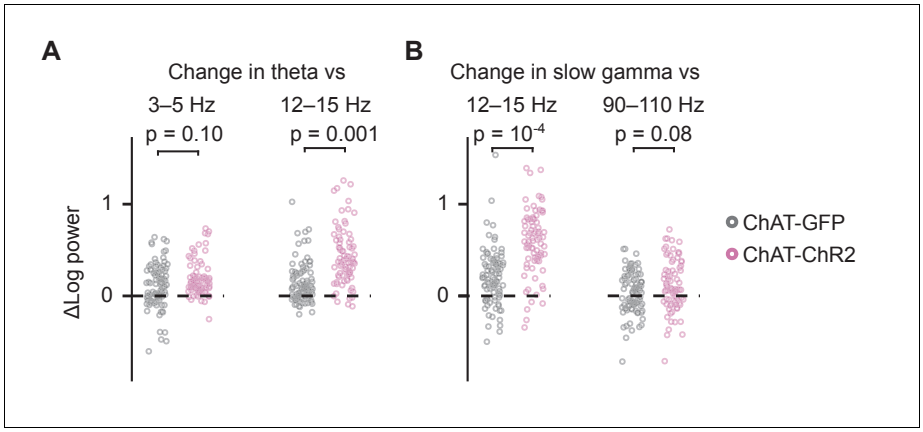

Figure 6—figure supplement 2. Power spectral density (PSD) change in theta and gamma vs. neighboring frequency band. (**A**) Change in theta power as the result of optogenetic stimulation compared to change in surrounding frequency bands. (**B**) As in (**A**) but for slow gamma power. Values are shown for log power differences in subsequent epochs with stimulation off and on. p vValues were calculated with linear mixed-effects models for the effect of the mouse group (ChAT-ChR2 vs. ChAT-GFP).